

# Preparation and Characterization of PLA Filaments for FDM 3D Printing

Amir Yusuf Mohd Shukri<sup>1</sup>, Abdul Manaf Abdullah<sup>1\*</sup>, Solehuddin Shuib<sup>1</sup>, Dasmawati Mohamad<sup>2</sup>

<sup>1</sup>School of Mechanical Engineering, College of Engineering, Universiti Teknologi MARA, 40450 Shah Alam, Selangor, Malaysia

<sup>2</sup>School of Dental Sciences, Health Campus, Universiti Sains Malaysia, 16500 Kubang Kerian, Kelantan, Malaysia

## ARTICLE INFO

### Article history:

Received 15 July 2024  
Revised 19 October 2024  
Accepted 23 October 2024  
Online first  
Published 15 January 2025

### Keywords:

Polylactic acid  
Fused deposition modelling  
Filament  
Extrusion  
Pulling speed

### DOI:

10.24191/jmeche.v22i1.4566

## ABSTRACT

Polylactic acid (PLA) is the predominant filament material utilised in fused deposition modelling (FDM) 3D printing. Despite being commonly utilised in FDM 3D printing, the fabrication of PLA filament involves a complex extrusion process that is not widely reported. This study aims to assess the thermal and melt flow behaviour of PLA. Besides, the impact of pulling speed on the resulting filament in terms of diameter, morphologies as well as mechanical properties was also quantified. The thermal behaviour of the PLA was evaluated using a thermogravimetric analyser and differential scanning calorimetry. Meanwhile, the flow rate of PLA was assessed using a melt flow indexer. The PLA was processed into a filament form using a single-screw extruder at three different pulling speeds of 500 rpm, 650 rpm, and 800 rpm, followed by an evaluation of its mechanical properties using a universal testing machine. The thermal properties data showed that the PLA started decomposing at 341 °C and melted at 170.9 °C. The melt flow rate of the PLA was 17 g/10 mins. The pulling speed of 500 rpm produced an optimal filament with a mean diameter of 1.785 mm. However, the strength and strain of the respected filament were slightly lower than those fabricated at pulling speeds of 650 rpm and 800 rpm. The ideal PLA filament was successfully fabricated at a pulling speed of 500 rpm. The findings from this study could be a stepping stone toward the fabrication of an enhanced PLA-based filament to be used for various applications.

## INTRODUCTION

Polylactic acid (PLA) is a member of the polyester family and composed of  $\alpha$ -hydroxy acids. PLA is a commonly used polymer owing to its biodegradability and biocompatibility. PLA is also considered a sustainable material as it can be produced using sustainable resources such as bamboo species as well as biomass feedstock like sugarcane. The mechanical properties of this polyester are relatively high. The tensile strength of PLA can reach 140 MPa and its tensile modulus ranges from 5 GPa to 10 GPa. However, it is brittle in nature with limited elongation of 3% under tensile conditions (Oksiuta et al., 2020). The production of PLA can be accomplished by three distinct methods, namely direct condensation polymerisation, azeotropic dehydrative, and lactide ring-opening polymerisation (ROP) (Avérous, 2008). Different routes will affect the structure of the PLA as well as its mechanical and thermal properties (Ramezani Dana & Ebrahimi, 2023).

Besides acrylonitrile butadiene styrene (ABS), the versatility of PLA made it a material of choice to be used for fused deposition modelling (FDM) 3D printing. Although the application of PLA for engineering applications is limited due to its resorbable and moisture absorption behaviour, these disadvantages somehow turn out to be advantageous to other applications such as tissue engineering (Hassanajili et al., 2019), where a 3D printed scaffold is expected to completely resorb over time and be replaced by a new hard tissue. Furthermore, in order to improve its biological performance, PLA is being combined with calcium phosphate-based materials. The prevalent materials for that particular purpose are typically hydroxyapatite and beta-tricalcium phosphate (Ferri et al., 2016; Marzuki et al., 2022). It should

<sup>1\*</sup> Corresponding author. *E-mail address:* [abdulmanaf@uitm.edu.my](mailto:abdulmanaf@uitm.edu.my)  
<https://doi.org/10.24191/jmeche.v22i1.4566>

be noted that the documented literature on PLA mainly focuses on the enhancement of its properties via the incorporation of fillers.

On the other hand, the quality of the filament feedstock is vital for an effective manufacturing process. The flowability of the filament as well as the filament diameter are among the factors that require attention. The filament diameter needs to be in the range of 1.65 mm to 1.85 mm to be grabbed by the rotated drive gear. In order to obtain the filament with the desired characteristics, a few factors such as barrel temperature, nozzle diameter and temperature, water bath distance (Hamat et al., 2023; Mishra et al., 2022), screw speed, and pulling temperature need to be taken into consideration during the filament fabrication process.

The influence of altering extrusion temperature and screw speed is once investigated where a temperature between 190 °C to 195 °C in combination with screw speed of 2 rpm to 5 rpm is reported to be optimum for producing a quality filament (Liu et al., 2017). While PLA is considered a common filament for FDM 3D printing, a thorough report on the filament fabrication or extrusion process for unfilled PLA is rather scarce, leaving a notable gap to be filled to further understand and improve the fabrication process. Moreover, different machine comes with their parameter setting which can substantially influence their performance and outcomes.

This study aims to assess the thermal behaviour and melt flow characteristics of the PLA. Besides, the effect of pulling speed during the filament extrusion process on the filament diameter was explored and the relationship between the variables was modelled. The strength of the obtained filament at varying pulling speeds was also measured and discussed.

## METHODOLOGY

The experimental approach to prepare and characterize the PLA filaments is illustrated in Fig 1.

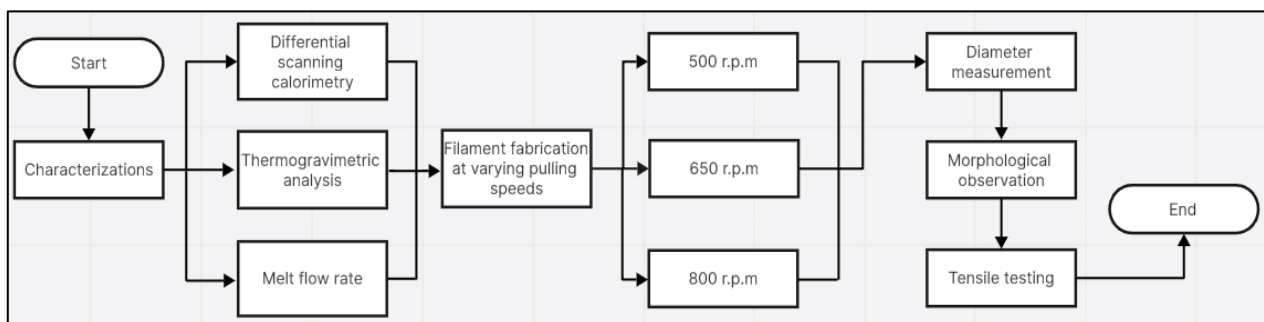


Fig. 1. Flowchart for preparation and characterization of PLA filament.

### Characterization of thermal properties and melt flow rate

In this study, PLA in pellet form was supplied by Pebblereka, Malaysia, having a density of 1.24 g/cm<sup>3</sup>. The thermal behaviour particularly relates to temperatures such as melting ( $T_m$ ), glass transition ( $T_g$ ), and heat of fusion ( $\Delta H_f$ ) of the PLA were determined using differential scanning calorimetry (Star System, Mettler Toledo, USA). Specifically, about 15 mg of PLA was deposited in an aluminium pan prior to the heat treatment process. The PLA was heated to 250 °C. The nitrogen gas flow rate was fixed at 20 mL/min and the heating rate was set at 10 °C/min. Meanwhile, the degree of crystallinity ( $X_c$ ) of the polymer was determined using Equation (1).

$$X_c = \frac{\text{Heat of fusion}}{\text{Polymer fraction} \times \text{melth enthalpy of PLA}} \quad (1)$$

The melting enthalpy of 100% crystalline polymer was taken as 93 J/g (Aliotta et al., 2022). Conversely, the initial and final decomposition temperature as well as the maximum decomposition temperature was ascertained using a thermogravimetric analyser (Star System, Mettler Toledo, USA). The sample was heated to 600 °C under 20 mL/min nitrogen gas flow. Then heating rate was also set at 10 °C/min. Meanwhile, the melt flow behaviour of the polymer was assessed using a melt flow indexer (MP 600, Tinius Olsen, USA). The indexer was heated to 190 °C prior to the experimentation. The release time was fixed at 300 sec and it was accomplished using 2.16 kg loads.

### Filament fabrication, morphological observation, and mechanical testing

Prior to the filament fabrication process, the PLA was desiccated overnight at 60 °C in a universal oven. The PLA was then fed into a hopper of a single screw extruder (SHS025, Songhu, China). The machine was equipped with three heating zones. The screw speed was set at 85 rpm while the first, second, and third heating zones were set at 195 °C, 198 °C, and 193 °C, respectively. The filament was fabricated at varying pulling speeds of 500 rpm, 650 rpm, and 800 rpm.

The diameter of the obtained filament was measured (100 readings at 20 mm intervals) using a vernier caliper. These measurements were slightly greater than previous research on the development of a new filament feedstock (Tuan Rahim et al., 2015). The morphological properties of the filament were analysed using a scanning electron microscope. The obtained filament was cut into 110 mm lengths for tensile testing using a universal testing machine (Servo pulser, Shimadzu, Japan). The gauge length was fit at 70 mm (Abdullah et al., 2018). The tensile test was conducted at a speed rate of 5 mm/min.

### Least square regression and statistical analysis

The correlation between the obtained filament diameter and the pulling speed was computed and modelled using a least square regression method. Least square is a well-established technique for simulating the sum of squared residuals in order to determine the best-fitting line. In detail, the computation was conducted using Equation (2), where  $n$  is the sample size,  $x$  is the pulling speed and  $y$  referred to filament diameter. Whereas  $a_0$  and  $a_1$  are coefficients representing the  $y$ -intercept and slope of the regression model, respectively.

$$\begin{pmatrix} n & \Sigma x \\ \Sigma x & \Sigma x^2 \end{pmatrix} \begin{pmatrix} a_0 \\ a_1 \end{pmatrix} = \begin{pmatrix} \Sigma y \\ \Sigma xy \end{pmatrix} \quad (2)$$

Meanwhile, the strength of the relationship between those parameters was statistically analysed using a Pearson correlation test. The test was computed at a significance level of  $p < 0.05$ .

## RESULTS AND DISCUSSION

### Thermal properties and melt flow rate

Fig 2 displays the DSC thermogram of PLA. Based on the obtained thermogram, two distinct peaks of 65.9 °C and 170.9 °C were detected which referred to glass transition and melting temperatures, respectively. Both temperatures differed by 1.7 °C - 2.5 °C as compared to those reported by Marzuki et al. (2022). However, it was in the range of temperatures reported by most of the literatures. The polymer chain undergoes motion at the glass transition temperature, resulting in an ultimate influence on the amorphous region. The shift from a rigid to a flexible state is anticipated to take place at that specific temperature. Meanwhile, the heat of fusion and crystallinity of the respected PLA were 5.58 J/g and 6.0 %, respectively (Table 1). It is worth noting that the PLA has a relatively low degree of crystallinity owing to its poor crystallization ability (Zhang et al., 2012). The crystallinity of a polymer plays a major function in ascertaining the mechanical characteristics of the polymer as it refers to the amount of ordered or aligned polymer chains with one another. Highly ordered polymer chain results in an improved rigidity which eventually enhances the mechanical properties such as tensile modulus (Ma et al., 2021).

The received PLA might be exposed to various treatments during processing prior to the shipment which affects its degree of crystallinity. It is well documented that thermal treatment such as water quenching results in rapid cooling which might affect the degree of crystallinity. Meanwhile, the amount of molecular weight yielded from the crosslinking of a polymer during polymerization process might also affect its crystallinity (Fulati et al., 2022). While the degree of crystallinity of the received polymer could not be controlled, methods such as annealing with optimized time and temperature could be opted to improve the respected property towards enhancement of its mechanical properties post-specimen fabrication (Srithep et al., 2013).

Conversely, the thermal profile of PLA is shown in Fig 3. Based on the obtained thermogram, PLA began decomposition at 341.9 °C, and the process concluded at 389.8 °C. The maximum decomposition temperature was recorded at 369.1 °C. No residue was quantified at the end of the heating, indicating that the received PLA was indeed a pure polymer. It is important to obtain the decomposition temperature as it could be used as a guide during the filament fabrication process.

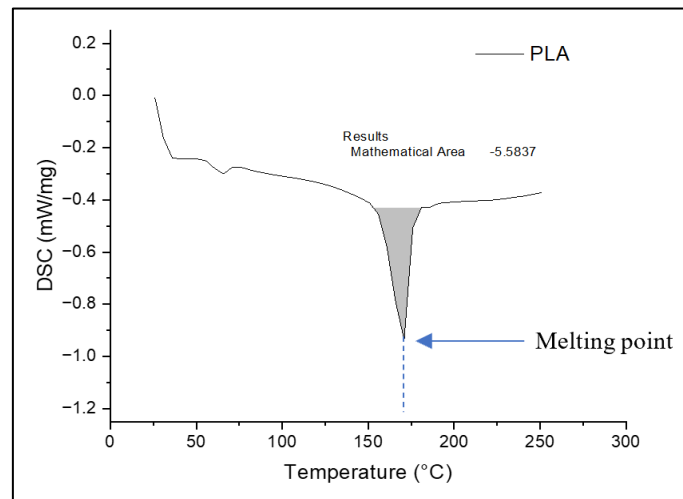


Fig. 2. DSC thermogram of PLA.

Table 1. Thermal properties calculated from DSC

Material	$T_g$ (°C)	$T_m$ (°C)	$\Delta H_f$ (J/g)	$\Delta H_f$ (J/g)
PLA	65.9	170.9	5.583	6.00

Particularly, the temperature during the filament fabrication needs to be set far below the decomposition temperature. Understanding the thermal stability profile of a polymer is crucial in order to set the processing window as well as ensure quality in manufacturing processes. While this study focuses on the unfilled PLA, it should be noted that the incorporation of fillers for instance might affect the thermal stability of PLA. Depending on the filler selection, the presence of carbonaceous fillers such as graphite in the PLA matrix seemed to reduce thermal stability. The filler facilitates the heat transfer resulting in the reduction of the decomposition temperature (Kaczor et al., 2021).

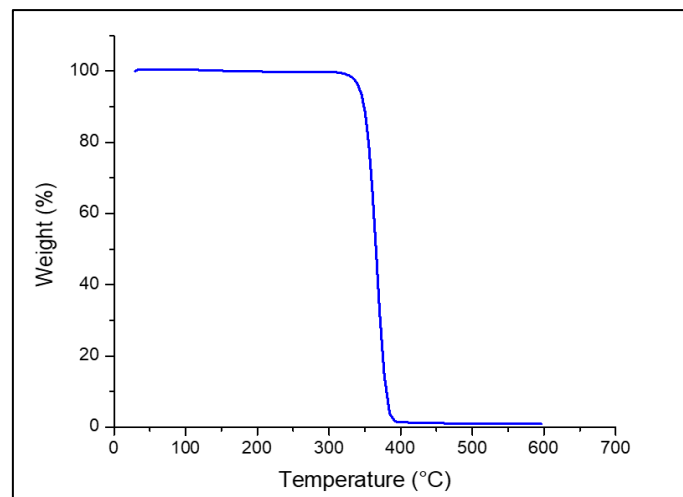


Fig. 3. TGA thermogram of PLA.

Meanwhile, the melt flow behaviour of the PLA is summarized in Table 2. The mean melt flow rate of PLA was 17.02 g/10 mins, measured at a 2.16 kg load at 190 °C. Understanding the flow rate of a polymer is deemed important for FDM 3D printing as it indicates the capability of the polymer to be melted and extruded through an orifice. The obtained melt flow rate was relatively higher than the other common filament feedstock such as acrylonitrile butadiene styrene (ABS). It is worth noting that the melt flow rate of ABS is 11 g/10 min under a higher load and temperature of 3.8 kg and 230 °C (SABIC, 2017).

Therefore, the melt flow rate of PLA as obtained in this study is considered appropriate for successful FDM 3D printing. Unlike other 3D printing methods, FDM 3D printing highly depends on the drive gear to grab and push the

filament to the extruding nozzle (Abdullah et al., 2017). A polymer with low flowability tends to affect the drive gear of the 3D printer.

Table 2. The melt flow rate of PLA specimens

Specimen	Final mass	Melt flow rate (g/10 mins)
1	0.45	17.00
2	0.46	16.25
3	0.47	17.51
4	0.46	14.32

### Fabricated filament and its diameter

The fabricated filament was measured to obtain its diameter. The fabricated filament and its normal distribution of the filament diameter at varied pulling speeds are presented in Fig 4. The mean diameter of the fabricated filament seemed to get bigger with the decrease in the pulling speed. The same trend was likewise noted in the standard deviation. The mean diameters of the filament were 1.35 mm, 1.62 mm, and 1.75 mm at the pulling speeds of 800 rpm, 650 rpm, and 500 rpm.

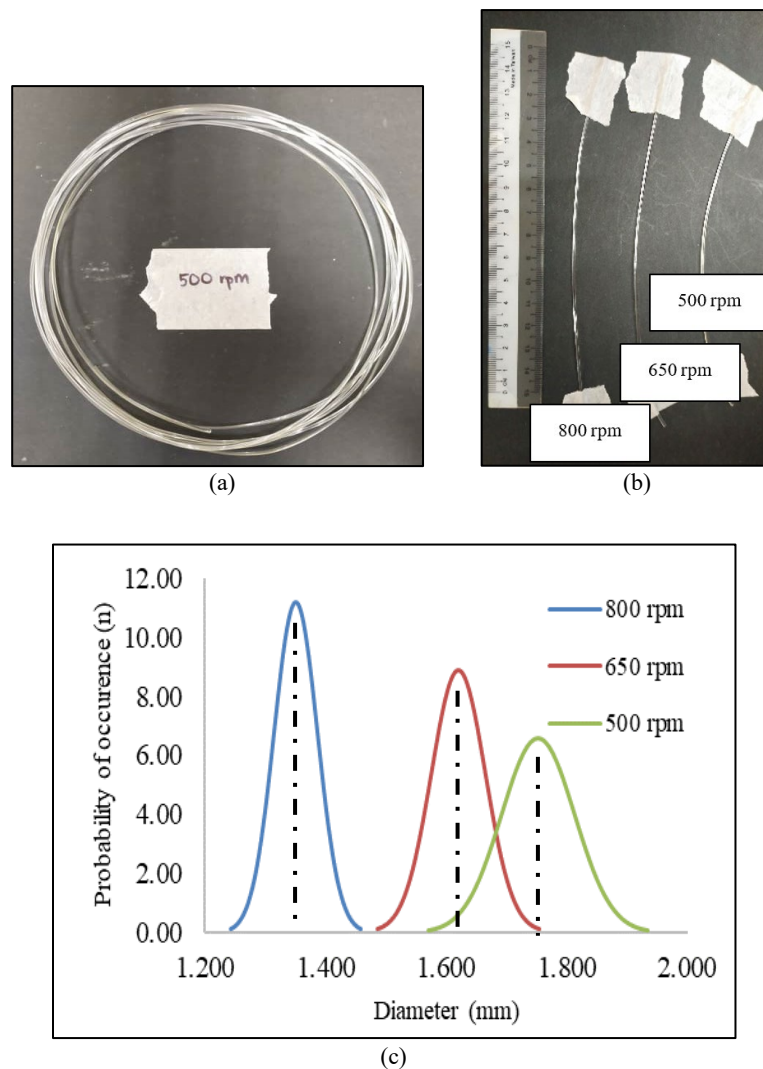


Fig. 4. Fabricated filament a) representative filament produced at 500 rpm, b) representative filament at different pulling speeds, and c) normal distribution of fabricated filament.

It should be noted that the diameter of the filament should range from 1.65 mm to 1.85 mm. Based on the obtained result, the pulling speed of 500 rpm produced filaments with the desired diameter. High pulling speed resulted in a thin

filament which was not suitable for FDM 3D printing. While a low speed seemed to be promising in the production of filament with the desired diameter, care should be taken as the speed might result in filament entanglement during the rapid cooling process in a water bath.

In this study, although filament fabrication at a pulling speed of 500 rpm was able to achieve the center diameter target of 1.75 mm, the resulting standard deviation was relatively larger than the other pulling speeds. Therefore, other considerations such as a combination of the particular pulling speed with other variables such as nozzle temperature need to be made in the future to reduce the standard deviation in order to obtain filament within the range of 1.65 mm to 1.85 mm. Other studies focusing on the filament fabrication of PLA using slightly different processing methods also indicated that multiple factors such as screw speed, cooling, and heating temperatures are crucial for obtaining a constant filament diameter (Hartig et al., 2021). Therefore, a systematic study that focuses on the response of the multiple parameters on the filament diameter could be suggested to reduce the standard deviation in order to obtain a filament diameter that falls within the specified range.

Fig 5 illustrates the correlation between pulling speed and filament diameter. Based on the obtained graph, the filament diameter and the pulling speed were almost inversely proportional to each other. A Pearson correlation test was performed to determine the correlation between the filament diameter and the rate of the pulling. The statistical analysis result revealed that there was a strong, negative, and highly significant correlation between the studied variables. The coefficient correlation value ( $r$ ) was -0.943 with  $p$  value of  $<0.001$ . It should be noted that the  $r$  value signifies the strength of the relationship, where an  $r$  value of more than 0.5 and 0.7 indicates moderate and strong relations, respectively.

A least square regression method was applied to determine the relationship between the variables as well as to establish a predictive model for prediction purposes. The established model is presented in Equation (3).

$$y = -0.0013x + 2.4448 \quad (3)$$

While this study aims at assessing the filament diameter at specific pulling speeds of 500 rpm, 650 rpm, and 800 rpm, the established model could be used to predict the filament diameter or to design a new experiment toward achieving a filament diameter with an improved accuracy.

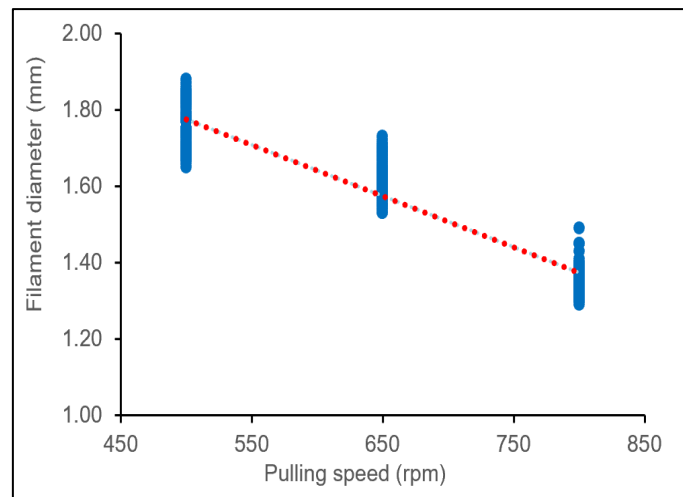


Fig. 5. The distribution of filament diameters at varied pulling speeds.

### Morphological properties

The obtained filament (1.75 mm in diameter) was manually fractured and morphologically examined via a scanning electron microscope. Based on the obtained microstructure, Fig 6, a rounded filament was observed indicating that the pulling speed of either 500 rpm, 650 rpm, or 800 rpm was able to produce a uniformly rounded filament. Besides, the rounded shape indicated that the extruded filament underwent sufficient cooling prior to the filament winding process. It should be noted that insufficient cooling might affect the shape of the filament, where an angular filament is expected with deviations in dimensions and structural integrity.

Meanwhile, the fractured surface of the filament was observed to further understand the potential behaviour of the filament. The surface was generally homogenous in nature. However small fragments and cracking were observed on the surface of the filament fabricated at a pulling speed of 500 rpm (Fig 6(a)) indicating the stress concentration point. It is anticipated that the filament is having low stress and strain based on the presence of the fragment and cracked structures. A relatively similar fragment was also observed in Fig 6(b), however no cracked structures were detected. Conversely, filament being pulled at 800 r.p.m exhibited a morphologically smoother surface with neither fragment nor cracking structures detected.

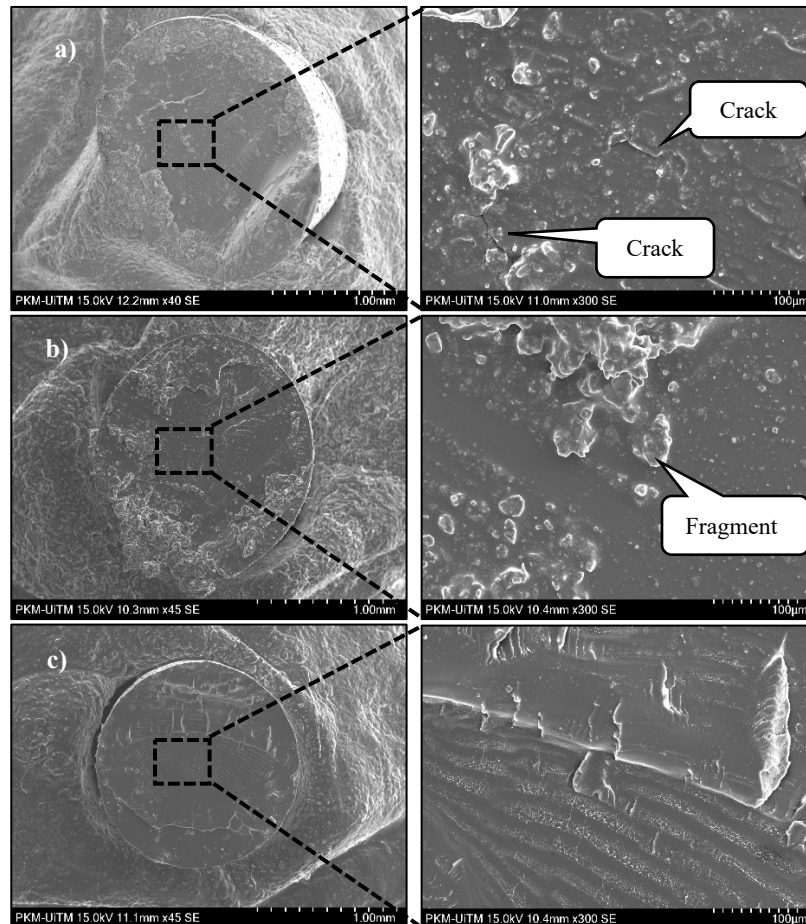


Fig. 6. Microstructure of fabricated filament at different pulling speeds a) 500 rpm, b) 650 rpm, and c) 800 rpm.

### Tensile properties

On the other hand, tensile testing was performed to ascertain the stress and strain, as well as to observe the behaviour of the obtained filament after being subjected to tensile forces. The mean tensile strength and strain of the filament are summarized in Table 3. Based on the obtained results, the highest strength and strain were recorded by the filament processes at a pulling speed of 800 rpm. It was then followed by 650 rpm and 500 rpm. The result was generally expected as the strength of the materials is highly dependent on their surface area, where a smaller surface area showed by a thinner filament tends to produce higher strength than thicker filaments. The strength of the 1.75 mm filament obtained at 500 rpm was half lower than the documented literature (Sivagnanamani et al., 2021). The strain was also reduced by 75%. The discrepancies in the obtained results as compared to the literature might occur due to the difference in the grade of the PLA.

Table 3. The tensile properties of the filament at various pulling speeds with standard deviation in parentheses

Pulling speed (rpm)	Tensile strength (MPa)	Tensile strain (%)
500	22.87 (1.805)	1.02 (0.181)
650	34.08 (5.853)	1.18 (0.001)
800	40.11 (8.045)	2.06 (0.137)

Besides strength, the strain value of the obtained filament is deemed important to be monitored. During the fabrication process, the extruded filament was pulled by a motor at certain speeds toward a winder. The semi-molten extruded filament was subjected to rapid cooling in a water bath prior to the spooling process. The gap between the nozzle and water level might delay the cooling process thus affecting the diameter of the filament as the motor continuously pulls the filament.

Meanwhile, the behaviour of the filament after subjected to tensile forces can be observed in Fig 7. The specimens generally exhibited an elastic deformation at the early stages. Lowering the pulling speed tended to reduce the value of the strain that caused the filament produced at that particular speed to fracture earlier than the others. However, it should be noted that the reduction of the pulling speed did not affect the winding process as the filament was still spool-able during the fabrication process. In contrast, filament fabricated at higher speed showed a markedly similar response at lower forces. Nevertheless, it had a steeper gradient than the others which led to a greater tensile modulus. It is anticipated that a higher pulling speed led to an improvement in the alignment of the polymer chain.

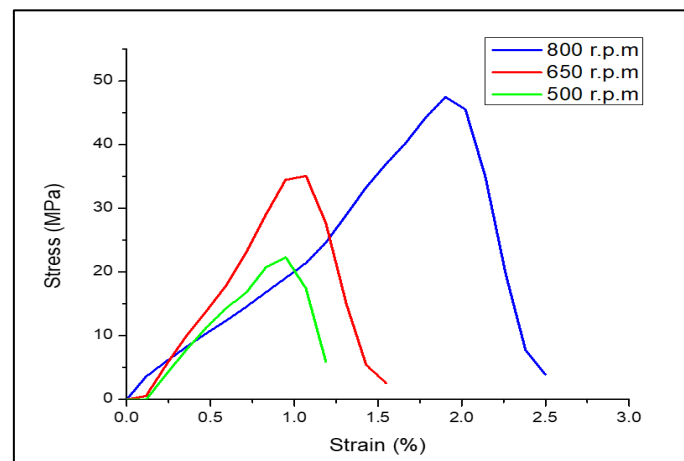


Fig. 7. Stress-strain graphs of PLA filament produced at varying pulling speeds.

The improvement in the molecular orientation enhances the ability of the filament to resist stress prior to catastrophic failure. Besides, well-aligned polymer chains are expected to effectively distribute the forces which reduce the probability of deformation under certain loads. The higher tensile properties exhibited by the filament fabricated under high pulling speed could also be attributed to the strain-hardening effects. It should be noted that filament fabricated at high pulling speed may experience such effects resulting in the enhancement in its yield stress which thereby allows the filament to endure high loads prior to permanent deformation. Thin filament with reduced diameter variability (Fig 4) tends to have a compact structure with reduced or non-detected defect site (Fig 6(c)), thus resulting in better tensile properties as compared to the filament with a bigger diameter, which explains the superior tensile properties shown by filament fabricated at fast pulling speed.

The stress-strain curves of the fabricated filament do not necessarily imply the behaviour of the 3D-printed part. However, to a certain extent, it can be utilised to forecast the mechanical characteristics of the 3D printed part. Up to date, there is no systematic study that summarizes the mechanical characteristics of the filament and the 3D printed part in a single study. Therefore, it would be interesting if the relationship between the mechanical behaviour of the filament and the 3D printed part could be elucidated in a future experimental setting.

## CONCLUSION

This study has successfully characterized the thermal and melt flow characteristics of the PLA and the effect of pulling speed on the filament diameter and its mechanical properties. The decomposition temperature of the PLA was significantly above its melting point, while the melt flow rate of the PLA surpassed that of typical filament feedstock such as ABS. The increase in the pulling speed typically reduces the filament diameter. The mechanical properties result showed that the diameter of the filament affects the stress and strain of the filament. This study identifies the lower and upper limits of pulling speed toward the fabrication of filament with the desired diameter. However, further refinement



is required to obtain a filament diameter with improved accuracy. Overall, this study could be a steppingstone towards understanding the filament fabrication process to develop an alternative range of PLA-based filaments.

## ACKNOWLEDGEMENTS/ FUNDING

The authors are grateful for the assistance of the College of Engineering, Universiti Teknologi MARA, in providing the thermal analysers and the School of Dental Sciences, Universiti Sains Malaysia, in providing the single screw extruder. The authors would like to thank Mrs Nora Aziz (Multidiscipline Laboratory, PPSG, USM) for her support during the experimentation. This research was made possible with funding from MyRA research grant 600-RMC 5/3/GPM (067/2022).

## CONFLICT OF INTEREST STATEMENT

The authors agree that this research was conducted in the absence of any self-benefits, commercial, or financial conflicts and declare the absence of conflicting interests with the funders.

## AUTHORS' CONTRIBUTIONS

The authors confirm their contribution to the paper as follows: **study conception and design:** Abdul Manaf Abdullah; **data collection:** Amir Yusuf Mohd Shukri; **analysis and interpretation of results:** Abdul Manaf Abdullah, Amir Yusuf Mohd Shukri; **draft manuscript preparation:** Amir Yusuf Mohd Shukri, Abdul Manaf Abdullah, Solehuddin Shuib and Dasmawati Mohamad. All authors reviewed the results and approved the final version of the manuscript.

## REFERENCES

- Abdullah, A. M., Tuan Rahim, T. N. A., Hamad, W. N. F. W., Mohamad, D., Akil, H. M., & Rajion, Z. A. (2018). Mechanical and cytotoxicity properties of hybrid ceramics filled polyamide 12 filament feedstock for craniofacial bone reconstruction via fused deposition modelling. *Dental Materials*, 34(11), e309-e316. <https://doi.org/https://doi.org/10.1016/j.dental.2018.09.006>
- Abdullah, A. M., Tuan Rahim, T. N. A., Mohamad, D., Akil, H. M., & Rajion, Z. A. (2017). Mechanical and physical properties of highly ZrO<sub>2</sub> / $\beta$ -TCP filled polyamide 12 prepared via fused deposition modelling (FDM) 3D printer for potential craniofacial reconstruction application. *Materials Letters*, 189, 307-309. <https://doi.org/https://doi.org/10.1016/j.matlet.2016.11.052>
- Aliotta, L., Sciara, L. M., Cinelli, P., Canesi, I., & Lazzeri, A. (2022). Improvement of the PLA crystallinity and heat distortion temperature optimizing the content of nucleating agents and the injection molding cycle time. *Polymers*, 14(5), 977. <https://www.mdpi.com/2073-4360/14/5/977>
- Av erous, L. (2008). Monomers, polymers and composites from renewable resources. In M. N. Belgacem & A. Gandini (Eds.), *Chapter 21 - Polylactic Acid: Synthesis, Properties and Applications* (pp. 433-450). Elsevier. <https://doi.org/10.1016/B978-0-08-045316-3.00021-1>
- Ferri, J., Gisbert, I., Garc a-Sanoguera, D., Reig, M., & Balart, R. (2016). The effect of beta-tricalcium phosphate on mechanical and thermal performances of poly(lactic acid). *Journal of Composite Materials*, 50(30), 4189-4198. <https://doi.org/10.1177/0021998316636205>
- Fulati, A., Uto, K., & Ebara, M. (2022). Influences of crystallinity and crosslinking density on the shape recovery force in poly( $\epsilon$ -Caprolactone)-Based shape-memory polymer blends. *Polymers*, 14(21), 4740. <https://www.mdpi.com/2073-4360/14/21/4740>
- Hamat, S., Ishak, M. R., Sapuan, S. M., Yidris, N., Hussin, M. S., & Abd Manan, M. S. (2023). Influence of filament fabrication parameter on tensile strength and filament size of 3D printing PLA-3D850. *Materials Today: Proceedings*, 74(3), 457-461. <https://doi.org/https://doi.org/10.1016/j.matpr.2022.11.145>

- Hartig, S., Hildebrandt, L., Fette, M., Meyer, T., Musienko, E., Redlich, T., & Wulfsberg, J. (2021). Process parameter determination for small recycling plants for the production of filament for FFF printing using the Taguchi method. *Progress in Additive Manufacturing*, 7(3), 87-97. <https://doi.org/10.1007/s40964-021-00218-x>
- Hassanajili, S., Karami-Pour, A., Oryan, A., & Talaei-Khozani, T. (2019). Preparation and characterization of PLA/PCL/HA composite scaffolds using indirect 3D printing for bone tissue engineering. *Materials Science and Engineering C, Materials for biological applications*, 104, 109960. <https://doi.org/10.1016/j.msec.2019.109960>
- Kaczor, D., Fiedurek, K., Bajer, K., Raszewska-Kaczor, A., Domek, G., Macko, M., Madajski, P., & Szroeder, P. (2021). Impact of the graphite fillers on the thermal processing of graphite/poly(lactic acid) composites. *Materials*, 14(18), 5346. <https://doi.org/10.3390/ma14185346>
- Liu, W., Zhou, J., Ma, Y., Wang, J., & Xu, J. (2017). Fabrication of PLA filaments and its printable performance. *IOP Conference Series: Materials Science and Engineering* (p. 012033). IOP Publishing Ltd. <https://doi.org/10.1088/1757-899X/275/1/012033>
- Ma, B., Wang, X., He, Y., Dong, Z., Zhang, X., Chen, X., & Liu, T. (2021). Effect of poly(lactic acid) crystallization on its mechanical and heat resistance performances. *Polymer*, 212, 123280. <https://doi.org/10.1016/j.polymer.2020.123280>
- Marzuki, A. P., Salleh, F. M., Rosli, M. N. S., Tharazi, I., Abdullah, A. H., & Halim, N. H. A. (2022). Rheological, Mechanical, and physical properties of poly-lactic acid (PLA)/ hydroxyapatites (HA) composites prepared by an injection moulding process. *Journal of Mechanical Engineering*, 19(2), 17-39. <http://dx.doi.org/10.24191/jmeche.v19i2.19669>
- Mishra, R., Bu Aamiri, O., Satyavolu, J., & Kate, K. (2022). Effect of process conditions on the filament diameter in single screw extrusion of natural fiber composite. *Manufacturing Letters*, 32(1), 15-18. <https://doi.org/https://doi.org/10.1016/j.mfglet.2022.01.003>
- Oksiuta, Z., Jalbrzykowski, M., Mystkowska, J., Romanczuk, E., & Osiecki, T. (2020). Mechanical and thermal properties of polylactide (PLA) composites modified with Mg, Fe, and Polyethylene (PE) additives. *Polymers*, 12(12), 2939. <https://www.mdpi.com/2073-4360/12/12/2939>
- Ramezani Dana, H., & Ebrahimi, F. (2023). Synthesis, properties, and applications of polylactic acid-based polymers. *Polymer Engineering & Science*, 63(1), 22-43. <https://doi.org/10.1002/pen.26193>
- SABIC. (2017). Technical data sheet Cycolac Resin MG 94. Saudi Arabia Basic Industries Corporation.
- Sivagnanamani, G. S., Begum, S. R., Siva, R., & Kumar, M. S. (2021). Experimental investigation on influence of waste egg shell particles on polylactic acid matrix for additive manufacturing application. *Journal of Materials Engineering and Performance*, 31(5), 3471-3480. <https://doi.org/10.1007/s11665-021-06464-y>
- Srithep, Y., Nealey, P., & Turng, L.S. (2013). Effects of annealing time and temperature on the crystallinity and heat resistance behavior of injection-molded poly(lactic acid). *Polymer Engineering & Science*, 53(3), 580-588. <https://doi.org/10.1002/pen.23304>
- Tuan Rahim, T. N. A., Abdullah, A. M., Md Akil, H., Mohamad, D., & Rajion, Z. A. (2015). Preparation and characterization of a newly developed polyamide composite utilising an affordable 3D printer. *Journal of Reinforced Plastics and Composites*, 34(19), 1628-1638. <https://doi.org/10.1177/0731684415594692>
- Zhang, J., Yan, D. X., Xu, J. Z., Huang, H. D., Lei, J., & Li, Z. M. (2012). Highly crystallized poly (lactic acid) under high pressure. *AIP Advances* 2(4), 042159. <https://doi.org/10.1063/1.4769351>